Molecular Biology of the Cell
Vol. 21, 2944–2952, August 15, 2010

Phosphatidic Acid Plays a Regulatory Role in Clathrin-mediated Endocytosis

Costin N. Antonescu, Gaudenz Danuser, and Sandra L. Schmid

Department of Cell Biology, The Scripps Research Institute, La Jolla, CA, 92037

Submitted May 11, 2010; Revised June 9, 2010; Accepted June 10, 2010
Monitoring Editor: Sandra Lemmon

Clathrin-mediated endocytosis (CME) is the main route of internalization of receptor-ligand complexes. Relatively little is known about the role of specific lipids in CME, in particular that of phosphatidic acid (PA). We examined the effect of altering cellular PA levels on CME by manipulating the activities and/or levels of either phospholipase D (PLD1 and PLD2) or diacylglycerol kinase (DGK), two enzyme classes involved in PA production. DGK inhibition resulted in a dramatic reduction of cellular PA, measured directly using an enzyme-coupled reaction, which resulted in a decreased rate of EGFR internalization measured biochemically. This corresponded to a decreased rate of clathrin-coated pit (CCP) initiation and increased lifetimes of productive CCPs, as determined by quantitative live-cell total internal reflection fluorescence microscopy. Unexpectedly, PLD inhibition caused an increase in cellular PA, suggesting that PLD activity negatively regulates PA synthesis by other more productive pathways. Consistent with opposite effects on cellular PA levels, PLD inhibition had opposite effects on EGFR internalization and CCP dynamics, compared with DGK inhibition. Importantly, the constitutive internalization of transferrin receptors was unaffected by either treatment. These findings demonstrate that PA plays a regulatory rather than obligatory role in CME and differentially regulates ligand-stimulated CME of EGFR.

INTRODUCTION

Clathrin-mediated endocytosis (CME) is the major pathway for internalization for receptor-ligand complexes from the cell surface in mammalian cells. Clathrin, together with cargo-binding adaptors such as AP-2 and numerous accessory proteins assemble to form an invaginating clathrin-coated pit (CCP), which then matures and pinches off to form a clathrin-coated vesicle (CCV; Conner and Schmid, 2003b; Schmid and McMahon, 2007). Phosphatidylinositol-(4,5)-bisphosphate (PIP_2) plays an obligatory, structural role in CME by acting as a membrane ligand for numerous CME proteins (Haucke, 2005). Whether other specific lipids function in CME remains less well understood.

A role for PLD, and hence its product phosphatidic acid (PA), in CME was suggested based on the observation that 1-butanol inhibits transferrin (Tfn) receptor (TfR) internalization (Boucrot *et al.*, 2006). Primary alcohols replace water in the phospholipase D (PLD)-catalyzed reaction leading to the formation of phosphatidyl-butanol instead of PA (Su *et al.*, 2009). Furthermore, expression of dominant-negative mutants of PLD and/or small interfering RNA (siRNA)-mediated gene silencing of PLD reduced the internalization of G-protein–coupled receptors (GPCRs) for angiotensin II (Du *et al.*, 2004) and μ-opioid (Koch *et al.*, 2004). PLD is recruited to the plasma membrane (PM) and potently is activated by binding to PIP_2 (Exton, 1997). In turn, the enzymatic activity of phosphatidylinositol-5-kinase type I, which produces PIP_2, is enhanced by PA. Together these findings suggest the existence of a positive feedback mechanism generating PA and PIP_2 (van den Bout and Divecha, 2009). Hence, PLD could have an obligatory function in CME, possibly through increasing synthesis of PIP_2.

However, recent findings based on siRNA-mediated gene silencing have suggested that PLD may not function in Tfn internalization (Padrón *et al.*, 2006; Lee *et al.*, 2009b), but is required for epidermal growth factor receptor (EGFR) internalization (Lee *et al.*, 2009b). Ligand-induced internalization of EGFR by CME is known to be mechanistically distinct from that of constitutively internalized receptors such as TfR (Sorkin and Goh, 2009). For example, CME of EGFR, but not TfR requires Grb2 (Jiang *et al.*, 2003) and CALM (Huang *et al.*, 2004), whereas perturbation of TTP (Tosoni *et al.*, 2005) and sequestration of AP2 by AAK1 overexpression (Conner and Schmid, 2003a) or depletion of AP2 (Motley *et al.*, 2003; Collinet *et al.*, 2010) perturbs TfR but not EGFR internalization. EGFR internalization requires activation of its tyrosine kinase activity (Lamaze and Schmid, 1995), and several residues within the cytoplasmic domain of EGFR become phosphorylated as a result of EGF treatment. However, it is still unclear which specific molecular signals link an activated EGFR to its rapid internalization via CME (Sorkin and Goh, 2009). Ligand binding by EGFR activates several protein and lipid signaling pathways, leading to an increase in PIP_2 degradation (van Rheenen *et al.*, 2007), as well as increased activities of enzymes that produce PA (Lee *et al.*, 2009a; Cai *et al.*, 2009). Hence, the observed selectivity of effects of PLD knockdown on EGFR internalization (Lee *et al.*, 2009b) might reflect differential requirements for certain lipids.

In addition to PLD, PA can also be produced by diacylglycerol kinase (DGK)-catalyzed phosphorylation of diacylglycerol (Cai *et al.*, 2009). siRNA-mediated gene silencing of DGKδ results in inhibition of both EGF and Tfn internalization (Kawasaki *et al.*, 2008), suggesting that PA produced in a PLD-independent manner might also contribute to CME. However, none of the studies that have explored the possi-

This article was published online ahead of print in *MBoC in Press* (http://www.molbiolcell.org/cgi/doi/10.1091/mbc.E10–05–0421) on June 23, 2010.

Address correspondence to: Sandra L. Schmid (slschmid@scripps.edu).

ble role of either PLD or DGK on CME has directly measured the effects of knockdown of these enzymes on cellular PA levels. Without knowing how perturbation of each enzyme alters PA levels, interpretations regarding the role of PA in CME may be premature.

We have reexamined the role of PA in CME of both EGFR and TfR and on the dynamic behavior of CCPs after siRNA-mediated knockdown and/or chemical inhibition of PLD and DGK activities and after direct measurement of cellular PA levels. Our findings provide new insight into the seemingly complex regulation of PA in cells and show that cellular PA levels play a selective regulatory role in clathrin-mediated endocytosis of EGFR.

MATERIALS AND METHODS

Cell Culture and Enzyme Inhibitors

Epithelial BSC-1 monkey kidney cells stably expressing clathrin light chain a (CLCa) fused to enhanced green fluorescent protein (CLCa–EGFP) were kindly provided by Dr. T. Kirchhausen (Harvard Medical School), and referred to simply as BSC-1 cells hereafter. Hep2 cells were kindly provided by Dr. Nathalie Sauvonnet (Institut Pasteur, France). All cells were grown in DMEM supplemented with 20 mM HEPES, 10 μg/ml streptomycin, 66 μg/ml penicillin, and 10% (vol/vol) fetal calf serum (FCS, Hyclone, Logan, UT), with the exception of Hep2 cells that were grown in DMEM supplemented with Glutamax (Invitrogen, Carlsbad, CA) and containing 10% (vol/vol) FCS, 10 μg/ml streptomycin, and 66 μg/ml penicillin. BSC-1 cells were additionally supplemented with 0.5 mg/ml G418 (Invitrogen). All cells were grown under 5% CO_2 at 37°C. Initial studies used 5-fluoro-2-indolyl-des-chlorohalopemide (FIPI) generously provided by Michael Frohman (SUNY, Stony Brook, NY), but in subsequent studies FIPI and R59949 were obtained from Sigma-Aldrich (St. Louis, MO).

Transfection of siRNAs and cDNAs

Transfection of BSC-1 cells with siRNA duplexes was performed using HiPerfect (Qiagen, Chatsworth, CA) according to the manufacturer's instructions and as previously described (Mettlen *et al.*, 2009). siRNA duplexes used were as follows: control siRNA was ON-Target*plus* nontargeting siRNA 1 (Dharmacon, Lafayette, CO), PLD1 (GGG AAG AAG GAG ACA GAA A, Qiagen), and PLD2 (AGA AAT ACC TGG AGA ATT A, Qiagen).

Transfection of cells with cDNAs was performed using Lipofectamine 2000 (Invitrogen), according to the manufacturer's instructions. After washing with OptiMEM to remove growth medium, BSC-1 cells were transfected using 2 μg DNA and 4 μl Lipofectamine 2000 in a total volume of 2 ml (per well of a six-cell plate) for 4 h. cDNA encoding the pleckstrin homology (PH) domain of PLCδ as well as a mutant of this domain that cannot bind to PIP_2 were previously described (Jost *et al.*, 1998) and subcloned in-frame into a GFP expression vector to generate GFP-PH-WT (wild type) and GFP-PH-mutant cDNAs. cDNA encoding the WT PA-binding sequence of Spo20 fused to GFP (GFP-PABD-WT), a mutant of GFP-PABD-WT that cannot bind to PA (GFP-PABD-mutant), and human PLD2, which we fused to mCherry (to generate mCherry-PLD2), were kind gifts of Dr. Michael A. Frohman.

Fluorescence Microscopy of Fixed Cells

In experiments to determine the plasma membrane localization of GFP-PH constructs, BSC-1 cells transfected with the indicated constructs were first detached by treatment with phosphate-buffered saline (PBS)/5 mM EDTA. Cells were then allowed to partially reattach on 22 × 22-mm glass coverslips for 15 min and then fixed in 4% paraformaldehyde (PFA) and mounted in Fluoromount G (Electron Microscopy Services, Hatfield, PA). Fluorescence images of cells were acquired by a Nikon TE300 inverted microscope (Melville, NY) with a CSU-22 confocal scanhead and a CoolSnapHQ camera (Photometrics, Tucson, AZ).

In experiments to examine the abundance of CCPs, BSC-1 cells stably expressing the AP-2 subunit σ2 fused to GFP (σ2-GFP) were fixed in 4% PFA and mounted in Fluoromount G (Electron Microscopy Services). Cells were then imaged using an Olympus IX71 epifluorescence microscope (Olympus, Center Valley, PA) with a Hamamatsu cooled CCD camera (Bridgewater, NJ).

Immunoblotting

To prepare whole cell lysates, cells grown on six-well plates were washed twice with cold PBS containing 1 mM $NaVO_4$ and then lysed by adding 100 μl of 2× Laemmli sample buffer (2× LSB: 0.125 M Tris, pH 6.8, 2% SDS [wt/vol], 5% glycerol [vol/vol], and 7.5% β-mercaptoethanol [vol/vol], supplemented with protease inhibitor cocktail [Sigma-Aldrich], 1 mM $NaVO_4$, and 100 nM okadaic acid). Lysed cells were scraped and transferred to a microfuge tube, passed through a 28-gauge syringe five times and then heated to 65°C for 20 min. Equal amounts of total protein of each sample were resolved by SDS-PAGE followed by immunoblotting as previously described (Mettlen *et al.*, 2009) using the following antibodies: rabbit polyclonal anti-EGFR (Santa Cruz Biotechnology, Santa Cruz, CA) and anti-PLD1 (Cell Signaling Technologies, Beverly, MA) and TD-1, a mouse monoclonal anti-clathrin (Transduction Laboratories, Lexington, KY), which was used for sample loading controls.

Quantitative RT-PCR Detection of PLD mRNA

Quantitative real-time (qPCR) experiments were performed using a Chromo 4 DNA Engine (Bio-Rad, Hercules, CA). After siRNA transfection of BSC-1 cells as indicated, RNA was purified by TRIZol-based extraction, as previously described (Chomczynski and Mackey, 1995). Specific primers for each of PLD1 (forward: TTC AAG GAG GTG TGG GTT TC; reverse: GTT CCT CCT CAG CTC GAA TG) and PLD2 (forward: AAA GGA CTG GAG GGG ATG AT; reverse: TCA AAG CCA GGG TCA AAG AG) were designed using Primer3 software (SimGene; http://www.simgene.com/Primer3;Rozen and Skaletsky, 2000). Specificity of primers was determined by searching against human and primate cDNA sequence databases of the National Center for Biotechnology Information. RT-PCR was performed using B-R-1-Step SYBR green qRT-PCR kit from Quanta (Gaithersburg, MD), according to the manufacturer's instruction. Standard curves for each primer set were constructed using serial dilutions of purified RNA from control BSC-1 cells. Initial validation of amplicons was performed by agarose gel electrophoresis to verify specific amplification of a single product of expected size. RT was performed by incubation at 50°C for 10 min and then 95°C for 5 min. PCR cycling was achieved by 40 cycles of 95°C for 10 s and 59°C for 1 min. A dissociation protocol was subsequently performed to verify the appropriate melting temperature and the presence of a single PCR product for each reaction. The amount of cDNA and hence initial mRNA present in each sample was calculated using Opticron Monitor 3.1.32 software (Bio-Rad) by the comparative threshold cycle (Ct) method and expressed as 2exp(Ct) using glucoronidase (forward primer: CTC ATT TGG AAT TTT GCC GAT T; reverse primer: CCG AGT GAA GAT CCC CTT TTT A) as an internal control. For determination of the relative amounts of mRNA in each sample, all conditions are expressed as a percentage of mRNA detected in control siRNA-treated cells.

Biochemical Internalization Assays

Tfn and EGF internalization assays were performed as previously described (Yarar *et al.*, 2005). Briefly, BSC-1 cells transfected as indicated and grown on 15-cm dishes were detached by incubation with PBS/5 mM EDTA and resuspended in PBS^{4+} (PBS supplemented with 1 mM $MgCl_2$, 1 mM $CaCl_2$, 5 mM glucose, and 0.2% bovine serum albumin [BSA]). Cells were then treated with inhibitors as indicated for 20 min at 37°C. For Tfn internalization, cells were then transferred to 4°C and surface-labeled with 1 μg/ml biotin-S-S-transferrin (BSST) for 45 min. Cells were then washed three times to remove unbound BSST and rewarmed for indicated times at 37°C. For EGF internalization, after incubation with inhibitors, cells were incubated with 2 ng/ml biotin-S-S-EGF (BSSE) at 37°C to allow internalization of BSSE for indicated times, after which cells were immediately placed at 4°C to arrest internalization. Cells were then washed to remove excess BSSE. Subsequently, surface-bound BSST or BSSE was quenched by sequential incubation with free avidin (0.05 mg/ml) and biocytin (0.05 mg/ml). Cells were then solubilized in blocking buffer (1% TX-100, 0.1% SDS, 0.2% BSA, 50 mM NaCl, and 1 mM Tris, pH 7.4), and cell lysates were plated onto ELISA plates coated with anti-transferrin (Scottish Antibody Production Unit, Carluke, Scotland) or anti-EGF (Upstate Biotechnology, Lake Placid, NY) antibody and assayed for detectable BSST or BSSE using HRP-labeled streptavidin as previously described (Yarar *et al.*, 2005; Liu *et al.*, 2008). Internalized BSST or BSSE was expressed as the percent of the total surface bound at 4°C (i.e., not quenched with avidin), measured in parallel.

PA Determination

The levels of cellular PA were measured using an enzyme-coupled fluorometric assay, as previously described (Morita *et al.*, 2009). Briefly, BSC-1 cells were detached by treatment with PBS/5 mM EDTA and resuspended in PBS^{4+}, treated or not with inhibitors for 20 min at 37°C, and then stimulated or not with EGF, as indicated. Cells were then immediately frozen or subjected directly to Bligh-Dyer lipid extraction (Bligh and Dyer, 1959). Total cellular lipids were incubated first with lipoprotein lipase of *Pseudomonas* sp. (Sigma-Aldrich) and then with glycerol-3-phosphate oxidase (Sigma-Aldrich) in the presence of horseradish peroxidase (Sigma Aldrich) and Amplex Red (Invitrogen). This resulted in the production of the fluorescent reporter resorufin in a PA-concentration–dependent manner (Morita *et al.*, 2009), as measured by fluorescence emission at 580 nm after excitation at 530 nm. For each experiment, a standard curve was generated using purified dioleylphosphatidic acid (Avanti Polar Lipids, Alabaster, AL) to ensure that [PA] determinations were made within a linear range with respect to resorufin fluorescence. PA detection was normalized to total protein content in the cellular sample determined before lipid extraction. Finally, in each experiment, [PA] values in treated cells were normalized to that of control cells.

Live Cell Total Internal Reflection Fluorescence Microscopy and Automated Image and CCP Lifetime Analysis

Fluorescent particle detection, lifetime tracking, and lifetime analysis of CCPs in BSC-1 cells stably expressing CLC-GFP was performed as previously described (Loerke *et al.*, 2009; Mettlen *et al.*, 2009). Imaging was performed on cells incubated in DMEM and 3% FCS.

Statistical Analyses

Measurements of Tfn or EGF internalization time courses under various conditions were subject to two-way analysis of variance (ANOVA) with Newman-Keuls post test, with $p < 0.05$ as a threshold for significant differences between treatments at a given time point. In addition, Tfn and EGF internalization measurements were normalized within each experiment to the corresponding control condition to yield % control endocytosis. Results from these assays, as well as measurements of cellular PA levels were subjected to one-way ANOVA with Newman-Keuls post test, with $p < 0.05$ as a threshold for significant difference among conditions.

Differences in CCP subpopulation lifetimes and percent contribution among various treatments were determined following a jackknife analysis of parameter uncertainty described previously (Mettlen *et al.*, 2009). Statistical analyses of differences among initiation density measurements were performed by Mann-Whitney rank sum test.

RESULTS

Inhibition of CME by 1-Butanol is PA- and PIP_2-independent

To begin to assess the contribution of PLD to CME, BSC-1 cells were treated with primary alcohols, used routinely to inhibit PLD. As reported previously (Boucrot *et al.*, 2006), Tfn internalization was potently inhibited by treatment with 1% 1-butanol (Figure 1A). Tfn internalization was also inhibited, albeit to a lesser extent, upon treatment with 1% 2-butanol, which is not expected to inhibit PLD (Figure 1A). Treatment of BSC-1 cells with lower concentrations of 1-butanol (0.1–0.25%) had little effect on Tfn internalization. This raised the concern that at least part of the inhibitory effect of 1% 1-butanol on CME might be independent of inhibition of PLD. We therefore directly measured the effect of 1-butanol on the cellular levels of PA. Surprisingly, treatment of BSC-1 cells with 1-butanol did not affect the levels of PA (Figure 1B); if anything there was a slight, albeit not significant increase in cellular PA levels. Of note, the assay used to measure PA is highly specific (Morita *et al.*, 2009); therefore it is unlikely that phosphatidylbutanol formed in cells incubated with 1-butanol contributes to PA measured. Thus, the inhibitory effects of 1-butanol appear not to be related to inhibition of PLD-catalyzed PA production.

The inhibitory effects of 1-butanol on CME have been ascribed to indirect effects on the production of PM-associated PIP_2 (Boucrot *et al.*, 2006). To test this possibility, we examined the effects of 1-butanol treatment on the localization of the PH domain of PLCδ fused to GFP (PH-GFP), a well-characterized PIP_2-binding probe (Stauffer *et al.*, 1998; Botelho *et al.*, 2000). BSC-1 cells treated with 1% 1-butanol for either 1 or 7 min exhibited a similar PM localization of PH-GFP as untreated control cells (Figure 1C, bottom panels). In contrast, in BSC-1 cells treated with phenylarsine oxide (PAO), an inhibitor of phosphatidylinositol-4-kinase that depletes PIP_2, or in cells expressing a PH-GFP mutant that cannot bind PIP_2, the fluorescent probe exhibited a diffuse cytosolic localization without enrichment at the PM (Figure 1C, top panels), validating the reliability of PH-GFP as a reporter. Therefore, it is unlikely that the inhibition of CME upon treatment with 1-butanol was due to a loss of bulk plasma membrane PIP_2.

It remained possible that a localized loss of PIP_2 in cells treated with 1-butanol resulted in the loss of membrane binding of CCP proteins. If so, the number of CCPs should decrease (Jost *et al.*, 1998; Zoncu *et al.*, 2007). Indeed, as previously reported (Boucrot *et al.*, 2006), upon initial treatment with 1-butanol BSC-1 cells stably expressing the GFP-labeled σ2 subunit of the tetrameric protein adaptor AP-2 (σ2-GFP) were rapidly depleted of visible GFP puncta corresponding to CCPs (Figure 1D, 1 min). However, upon prolonged incubation with 1-butanol (>7 min), BSC-1 cells regained CCPs to levels comparable to control (Figure 1D, 7 min). In contrast, and as expected, BSC-1 cells treated with

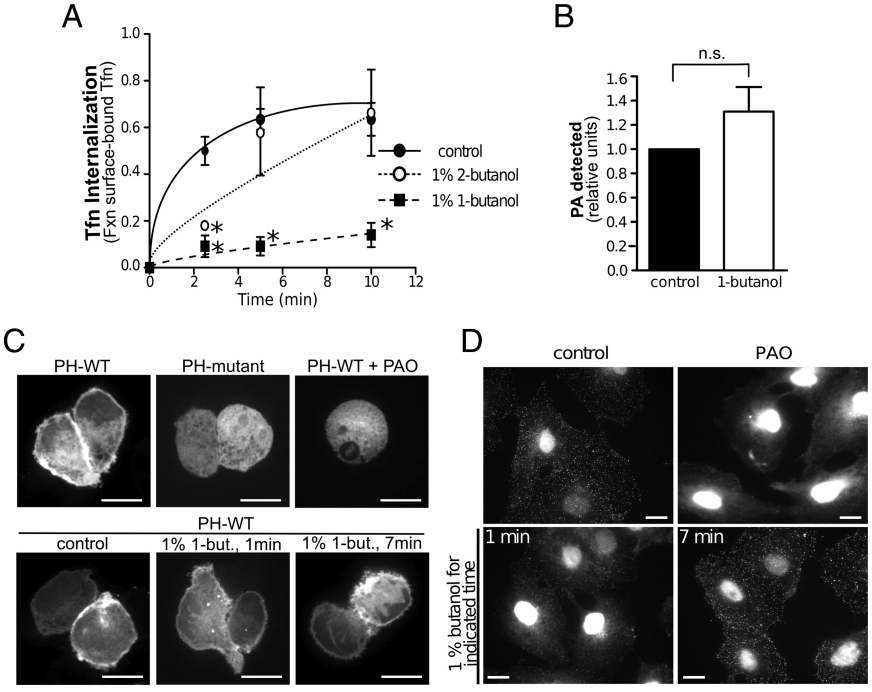

Figure 1. Primary and secondary alcohols inhibit CME. (A) Tfn internalization was measured in BSC-1 cells treated with either 1- or 2-butanol (1%, vol/vol) for 20 min or left untreated (control), as indicated. Shown are the means ± SE of 3–5 independent experiments. * $p < 0.05$, relative to corresponding time point of the control condition. (B) PA levels were determined in cells either treated with 1% 1-butanol for 20 min or left untreated (control). Shown are the means ± SE of three independent experiments. (C) BSC-1 cells transfected with GFP-PH WT or PIP_2-binding deficient mutant were treated as indicated, rounded-up and imaged as described in *Materials and Methods*. Shown are fluorescence micrographs representative of at least 2 independent experiments. (D) BSC-1 cells stably expressing σ2-GFP were treated as indicated, fixed and then imaged as described in *Materials and Methods*. Shown are fluorescence micrographs representative of 3 independent experiments. Scale bars 10 μm.

PAO and hence depleted of PIP_2 exhibited a dramatic and persistent loss of CCPs.

From this we conclude that the observed inhibition of CME in BSC-1 cells by 1-butanol is not due to changes in cellular PA or PIP_2 levels and may not be related to inhibition of PLD. Primary alcohols have been used extensively to inhibit PLD in cells; however, there appears to be a growing list of biological phenomena that are sensitive to inhibition by primary alcohols but not other methods of perturbing PLD (Su *et al.*, 2009; Scott *et al.*, 2009; Yanase *et al.*, 2010). The results presented here strongly suggest that 1-butanol inhibits CME via PLD-independent mechanisms. Therefore, to assess the contribution of PLD to CME, more specific methods of perturbation of this enzyme must be used.

PLD Inhibition Increased Cellular PA and Increased EGFR Internalization and CCP Turnover

Recently, FIPI was shown to be a specific PLD inhibitor that does not exhibit some of the off-target effects of primary alcohols (Su *et al.*, 2009). In contrast to the effects of 1-butanol, treatment of BSC-1 cells with FIPI had no significant effect on the initial rate of Tfn internalization (Figure 2A). Given previous reports of effects of PLD inhibition of ligand-induced internalization events (Du *et al.*, 2004; Koch *et al.*, 2004; Lee *et al.*, 2009b), we measured the internalization of EGF. We used low concentrations of ligand (2 ng/ml) to ensure selective uptake via CME (Sigismund *et al.*, 2008). Under these conditions, EGF internalization appeared to be slightly elevated (n = 7) in cells treated with FIPI compared with control (Figure 2B). These differences were consistent over multiple independent experiments. To illustrate this, we normalized the extent of Tfn or EGF internalization after 2 min to that of control cells within each experiment. These data revealed that FIPI treatment resulted in a significant increase in the initial rate of EGF internalization (141.1 ± 14.8% vs. control, n = 7, $p < 0.05$), without affecting Tfn internalization (Figure 2C).

To determine whether the effect of FIPI on EGF internalization correlated with changes in cellular PA levels, we measured these directly (Figure 2D). Surprisingly, FIPI treatment resulted in a small but significant increase in PA levels. Control experiments in cells overexpressing PLD and thus overproducing PA, confirmed that FIPI indeed inhibited cellular PLD activity at this concentration (see Supplemental Figure 1). Thus, we conclude that inhibition of endogenous PLD by FIPI resulted in a small, but significant increase in both cellular PA levels and the rate of EGF internalization.

Given the small effects of FIPI on EGF internalization, we used an additional, more sensitive assay to determine the effect of the drug on CME. To study CCP maturation, we

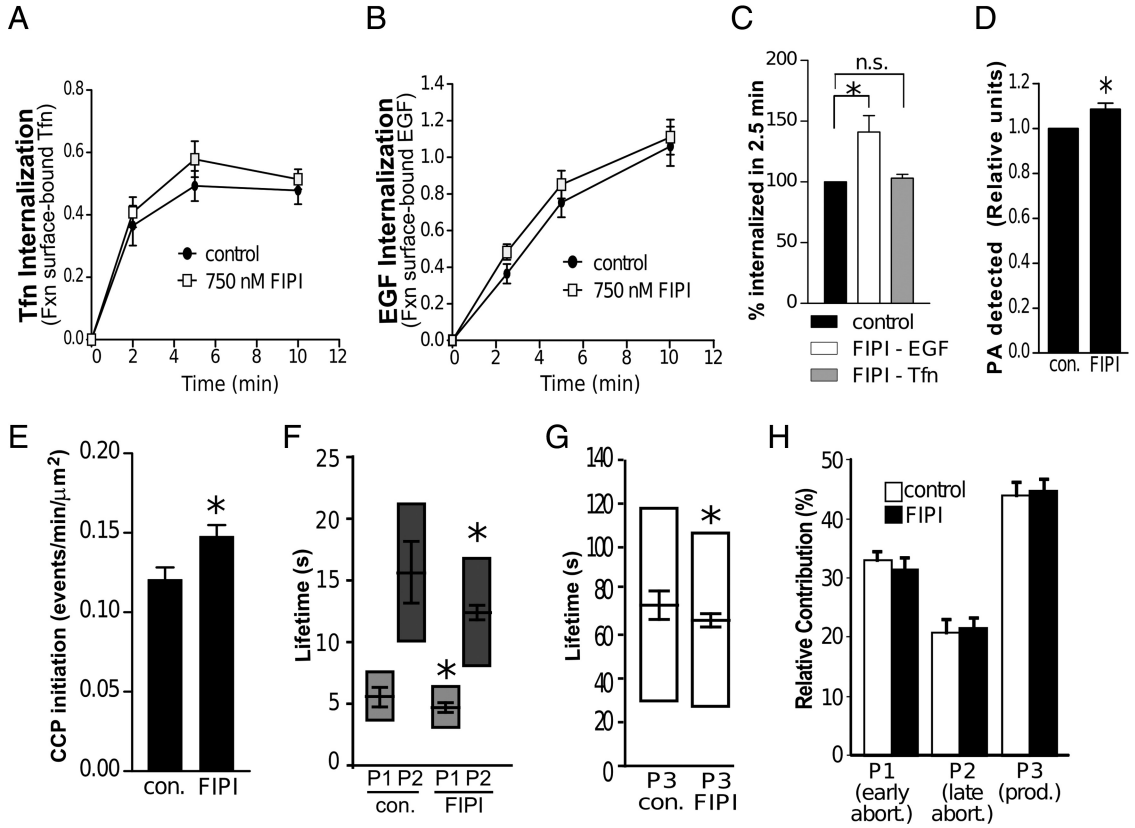

Figure 2. FIPI enhances EGF internalization, PA levels and CCP initiation and turnover. Tfn (A) or EGF (B) internalization was measured in BSC-1 cells treated with 750 nM FIPI or vehicle only (0.1% DMSO, control), as indicated. Shown are the means ± SE of seven independent experiments. (C) The amount of Tfn or EGF internalized was normalized and expressed as a percentage of that seen in corresponding control cells in each experiment. Shown are the means ± SE of seven independent experiments. *$p < 0.05$. (D) PA levels were determined in cells treated as in A compared with control. Shown are the means ± SE of nine independent experiments. *$p < 0.05$. (E–H) The results of TIR-FM imaging and CCP lifetime decomposition in cells treated or not with 750 nM FIPI are shown. (E) CCP initiation rate, lifetimes of CCP abortive (F) and productive (G) subpopulations and (H) relative contributions of CCP subpopulations. Error bars, cell-to-cell variation; the length of the lifetime bars in F and G denotes the t_{50}-spread of the distribution. The number of CCP trajectories (n) and cells (k) for each condition are control (DMSO): n = 40557, k = 30; and FIPI: n = 31875, k = 30. (E) *$p < 0.05$, (F–H) *$p < 10^{-8}$.

have recently developed an assay that tracks a large number of CCPs ($n > 10,000$) in time-lapse images obtained by total internal reflection fluorescence microscopy (TIR-FM) of cells expressing CLC fused to GFP, enabling rigorous and automatic quantitation of CCP lifetimes. This method has revealed that CCPs are highly heterogeneous with respect to their lifetime (Loerke *et al.*, 2009) and size (Mettlen *et al.*, 2010) and that CCPs exist in three dynamically distinct subpopulations: two short-lived abortive subpopulations (termed P1 and P2) hypothesized to be transient, nonproductive events and a longer-lived productive subpopulation (termed P3) leading to CCV formation (Loerke *et al.*, 2009). Using this assay, we have found that siRNA silencing of various endocytic accessory proteins resulted in diverse and discernable effects on CCP dynamics, even under conditions in which little or no change in cargo internalization could be detected biochemically (Mettlen *et al.*, 2009). We therefore used this more sensitive method to examine the effects of specific cellular perturbations on the dynamic behavior of CCPs. Importantly, cells are maintained in 3% serum, which contains growth factors such as EGF during the acquisition of TIR-FM movies.

Consistent with the observed increase in EGFR internalization rates, treatment of BSC-1 cells with FIPI resulted in an increase in the rate of CCP initiation (Figure 2E) and a reduction of the lifetimes of abortive (Figure 2F) as well as productive CCPs (Figure 2G). The relative contribution of the productive (P3) subpopulation of CCPs was unaffected (Figure 2H). Of note, FIPI only affects the uptake of EGF but not Tfn (Figure 2D). Therefore, its effects on overall CCP dynamics are likely to be an underestimation of the specific effects of the drug on the EGFR-containing subset of CCPs.

If the effects of FIPI treatment on CME were indeed due to a specific inhibition of PLD, then siRNA gene silencing of PLD1 and PLD2 in BSC-1 cells should give a similar phenotype. Transfection of BSC-1 cells with both PLD1- and PLD2-specific siRNAs together resulted in a reduction of 61.6 ± 9.1% ($n = 5$, $p < 0.05$) and 63.7 ± 6.9% ($n = 6$, $p < 0.05$) of their corresponding mRNAs, respectively (Figure 3A, left panels). Although reliable specific antibodies to PLD2 are currently unavailable (Scott *et al.*, 2009), we were able to confirm a corresponding reduction in PLD1 protein (Figure 3A, right panel). Consistent with the FIPI results, siRNA gene silencing of PLD1 and PLD2 had no affect on Tfn internalization (Figure 3B), but EGF internalization was consistently elevated ($n = 3$; Figure 3C). We again normalized the extent of Tfn and EGF internalization to control within each experiment to show that siRNA knockdown of PLD1 and 2 resulted in a significant (163.7 ± 60.1% vs. control, $n = 3$, $p < 0.05$) and specific increase in EGF internalization (Figure 3D). Thus we conclude that inhibition of PLD specifically increases the internalization of EGFR, suggesting that PLD may negatively regulate a cargo-selective subset of CCPs.

These results were further confirmed by examining the effect of siRNA-mediated gene silencing on CCP dynamics.

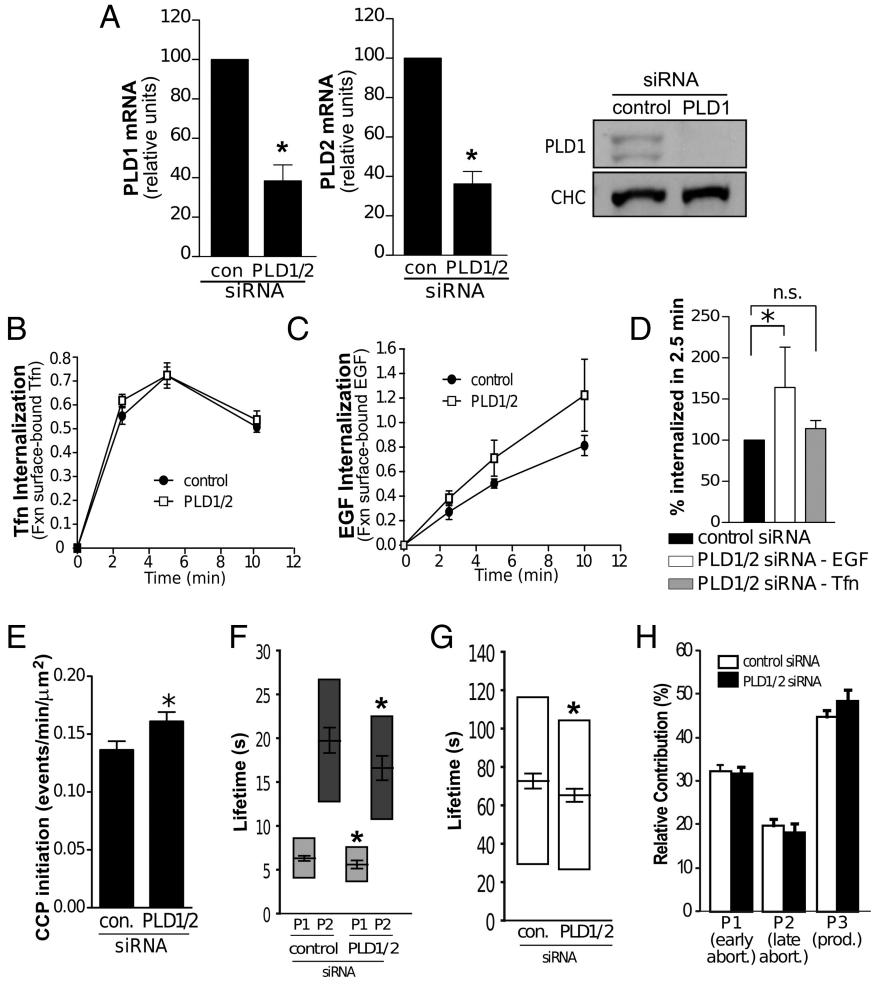

Figure 3. siRNA silencing of PLD1/2 enhances EGF internalization, PA levels and CCP initiation and turnover. (A) BSC-1 cells transfected with siRNA targeting PLD1 and PLD2 or control siRNA and were subjected to RNA isolation and qRT-PCR detection of PLD1 and PLD2 mRNA content (left panels, means ± SE of 5–6 independent experiments ($*p < 0.05$) or to immunoblotting with PLD1-specific antibodies (right panel, an immunoblot representative of four independent experiments). Tfn (B) or EGF (C) internalization was measured in BSC-1 cells treated with siRNA targeting PLD1/2 or control siRNA, as indicated. Shown are the means ± SE of 3–5 independent experiments. (D) The amount of Tfn or EGF internalized was normalized and expressed as a percentage of that seen in control cells in each experiment. Shown are the means ± SE of 3–5 independent experiments. $*p < 0.05$ (E–H) Results of TIR-FM imaging and CCP lifetime decomposition in cells treated with either control or PLD1/2 siRNAs are shown. (E) CCP initiation rate, lifetimes of CCP abortive (F) or productive (G) subpopulations and (H) relative contributions of CCP subpopulations. Error bars, cell-to-cell variation; the length of the lifetime bars in F–G denotes the t_{50}-spread of the distribution. The number of CCP trajectories (n) and cells (k) for each condition are control siRNA: $n = 50692$, $k = 40$; and PLD1/2 siRNA: $n = 49491$, $k = 30$. (E) $*p < 0.05$, (F–H) $*p < 10^{-8}$.

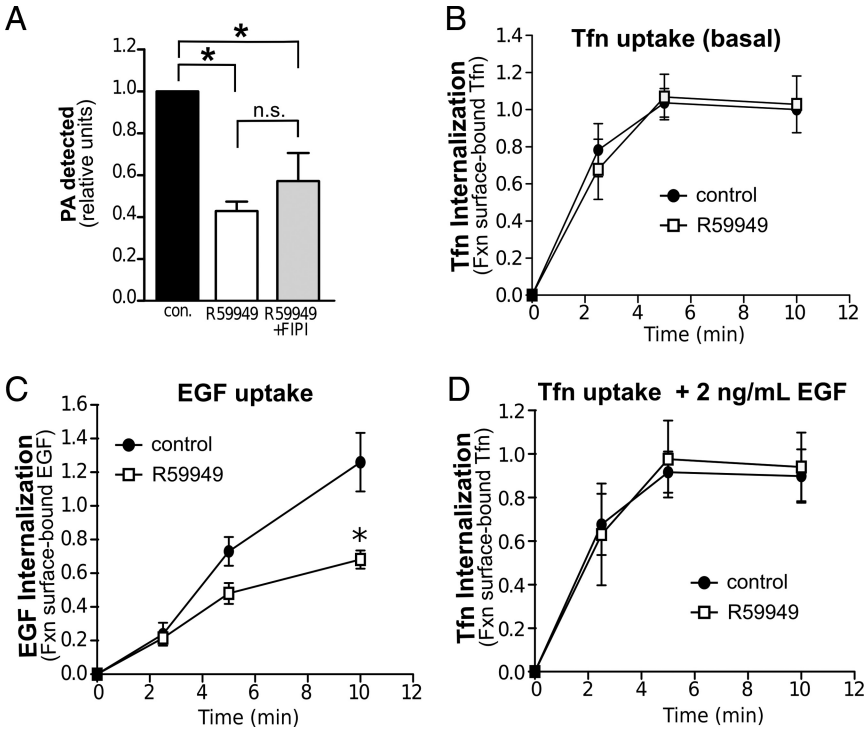

Figure 4. Inhibition of DGK reduces cellular PA levels and inhibits EGF but not Tfn internalization. (A) BSC-1 cells were treated with the DGK inhibitor R59949 (30 μM) with or without the PLD inhibitor FIPI (750 nM) or left untreated (0.1% DMSO vehicle, control) for 20 min as indicated before determining the cellular PA content. Shown are the means ± SE of seven independent experiments *$p < 0.05$. (B) Tfn or (C) EGF internalization or (D) Tfn internalization in the presence of unlabeled 2 ng/ml EGF was measured in BSC-1 cells treated or not with 30 μM R59949 as indicated. Shown are the means ± SE of six independent experiments. *$p < 0.05$, relative to corresponding time point of the control condition.

As for FIPI treatment, siRNA knockdown of PLD1 and PLD2 in BSC-1 cells resulted in an increase in CCP initiations (Figure 3E) and a reduction of the lifetimes of both abortive (P1 and P2; Figure 3F) and productive (P3) CCPs (Figure 3G). There was no effect of PLD1 and 2 silencing on the relative contributions of productive CCPs (Figure 3H). Thus, both acute (FIPI) and prolonged (siRNA-mediated silencing of PLD1/2) inhibition of PLD resulted in strikingly similar, selective increases in EGFR internalization, CCP initiation, and turnover rate of both abortive and productive populations of CCPs.

DGK Inhibition Decreased Cellular PA and Reduced EGFR Internalization and CCP Turnover

The product of PLD, PA, can be produced by other enzymatic reactions, including by DGKs that catalyze phosphorylation of diacylglycerol. We therefore measured the contribution of these enzymes to total cellular PA levels. Treatment of cells with the class I DGK inhibitor R59949 resulted in a dramatic reduction (to 42.8 ± 4.8% of control) of total PA levels (Figure 4A). When added in the presence of R59949, FIPI did not further reduce PA levels (Figure 4A) and indeed produced a slight, although not significant increase. Similar results were obtained in HeLa cells (data not shown) and in human embryonic kidney (HEK) 293 cells (Morita *et al.*, 2009). Together, these data suggest that type I DGKs contribute the majority of total cellular PA levels.

As DGKs control the levels of total cellular PA, we examined the contribution of this lipid kinase to Tfn and EGF internalization. Treatment with R59949 did not affect Tfn internalization (Figure 4B), but resulted in a robust inhibition of EGF internalization (Figure 4C). Importantly, treatment of cells with EGF at the same concentration used to measure EGF internalization (2 ng/ml) did not result in sensitization of Tfn internalization to R59949 (Figure 4D). This result provides strong evidence that R59949 is specifically inhibiting EGF, but not Tfn internalization, as opposed to affecting CME more generally, but only in EGF-stimulated cells.

We next determined the effect of inhibition of class I DGKs on CCP dynamics. Consistent with the observed decrease in EGFR internalization rates, BSC-1 cells treated with R59949 exhibited a decrease in CCP initiation (Figure 5A) and a

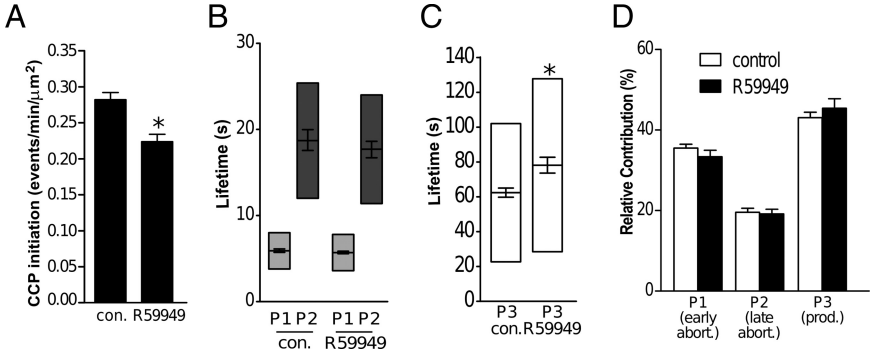

Figure 5. Inhibition of DGK reduces CCP initiation and turnover of productive CCPs. Results of TIR-FM imaging and CCP lifetime decomposition in cells treated or not with 30 μM R59949 are shown. (A) CCP initiation rate, lifetimes of (B) abortive or (C) productive CCP subpopulations and (D) relative contributions of CCP subpopulations. Error bars, cell-to-cell variation; the length of the lifetime in panels B and C denotes the t_{50} spread of the distribution. The number of CCP trajectories (n) and cells (k) for each condition are control (DMSO): n = 136847, k = 38; and R59949: n = 117965, k = 41. (A) *$p < 0.05$ (B–D) *$p < 10^{-8}$.

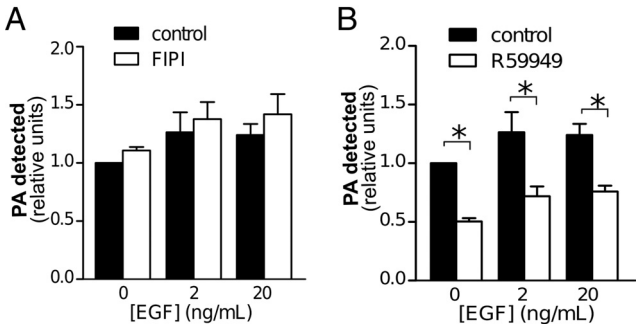

Figure 6. EGF treatment does not affect the reduction of PA levels due to inhibition of DGK. BSC-1 cells were treated with either (A) the PLD inhibitor FIPI (750 nM) or (B) the DGK inhibitor R59949 (30 μM) or left untreated (0.1% DMSO vehicle, control) for 20 min as indicated and then stimulated or not with EGF, as indicated for 5 min. Cells were then immediately subject to extraction of lipids and determination of cellular PA content. Shown are the means ± SE of six independent experiments. *$p < 0.05$.

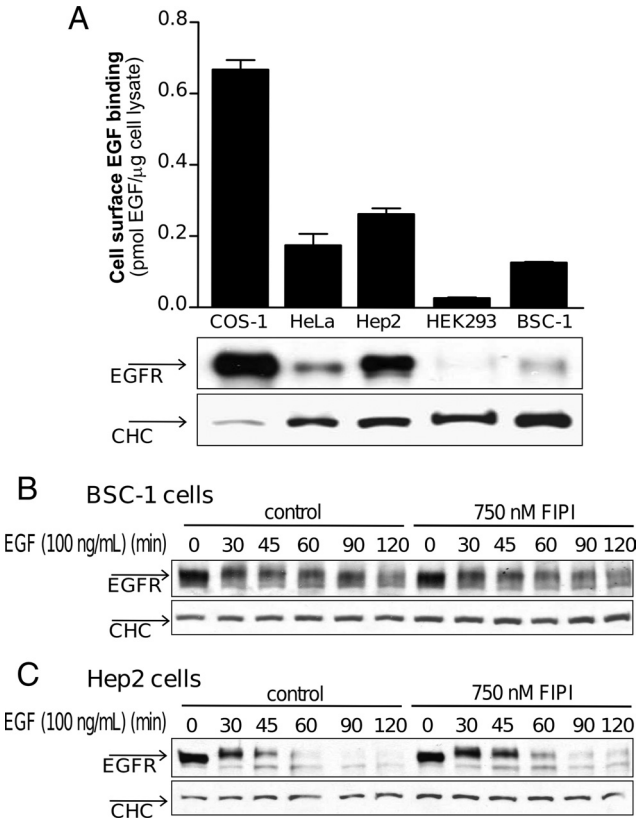

Figure 7. FIPI treatment leads to delay of EGFR degradation. (A) Cell surface EGF binding and EGFR expression levels were determined in COS-1, HeLa, HEK293, Hep2, and BSC-1 cells, as indicated. Shown are the means of at least four independent EGF cell surface–binding experiments, as well as an anti-EGFR immunoblot representative of four independent experiments. Membranes were subsequently probed with anti-CHC antibodies as a loading control. BSC-1 (B) or Hep2 (C) cells were treated with 750 nM FIPI or vehicle control (DMSO) for 20 min and then stimulated or not with 100 ng/ml EGF for the indicated time. Whole cell lysates of each condition were subject to immunoblotting with anti-EGFR antibodies. Membranes were subsequently probed with anti-CHC antibodies as a gel loading control.

specific increase in the lifetime of productive (P3) CCPs (Figure 5, B and C) without affecting the relative contribution of productive CCPs within the total CCPs detected (Figure 5D). Notably, the effects of treatment with R59949 on CCP dynamics were qualitatively opposite to those of FIPI treatment or siRNA-mediated PLD silencing. Together our results suggest that Tfn and EGF internalization via CME can be differentiated by the dependence on DGK-generated PA levels and that the internalization of each cargo is largely independent of the other. These data strengthen our conclusion that PA levels play a selective regulatory role in CME of EGFR.

EGF stimulation has been reported to increase both PLD (Lee *et al.*, 2009a) and DGK (Cai *et al.*, 2009) activities. Therefore, it remained possible that EGF stimulation changes the contribution of each enzyme to cellular PA levels, thereby accounting for the differential effects of these perturbations on EGF uptake. However, in cells stimulated for 5 min with either 2 or 20 ng/ml EGF, we did not observe a statistically significant increase in total PA levels (Figure 6). Moreover, the effects of FIPI and R59949 on PA levels were unchanged when cells were stimulated with EGF. Thus, although EGF stimulation may result in an increased activity of PLD and/or certain DGKs, this appears to contribute a negligible amount of PA relative to that produced constitutively, largely through class I DGKs. Hence, regardless of EGF stimulation, PLD has a minor and negative contribution toward total cellular PA levels, whereas DGK type I are the major contributors to total cellular PA levels.

PLD Inhibition Delays EGFR Degradation

In addition to their effects on EGFR internalization, expression of WT- and dominant-negative PLD were previously shown to increase and decrease the rate of EGFR degradation, respectively (Shen *et al.*, 2001). Given our unexpected finding that acute inhibition of PLD activity by FIPI treatment enhances PA levels and EGF internalization, we also examined the effect of FIPI treatment on EGFR degradation. Compared with other commonly used cell lines, BSC-1 cells express low, but clearly detectable levels of EGFR, as measured by either cell surface binding of EGF or immunoblotting (Figure 7A). In the presence of 100 ng/ml EGF, the EGFR was degraded slowly after internalization into BSC-1 cells, and this rate did not appear to be affected by FIPI treatment (Figure 7B). We therefore examined the effect of FIPI on EGFR internalization and degradation in Hep2 cells, which express higher levels of EGFR (Figure 7A) and exhibit a faster rate of EGFR degradation (Figure 7C). As for BSC-1 cells, FIPI treatment of Hep2 (and all other cell lines examined) resulted in a slight increase in the rate of EGF internalization (data not shown). In Hep2 cells we also detected a delay in EGFR degradation upon treatment with FIPI (Figure 7C). Hence, we were able to confirm a role for PLD activity in EGFR degradation. These results suggest that some localized production of PA by PLD, likely on intracellular membranes, may contribute to EGFR trafficking to the lysosome.

DISCUSSION

We have found that manipulations of PLD and DGK, enzymes that regulate PA biosynthesis, differentially and selectively affect clathrin-mediated endocytosis of EGFR, without affecting TfR internalization. Previous studies have explored the effect of manipulation of either PLD or DGK

activities on CME, but have not directly determined whether these manipulations affect cellular PA content. We find that inhibition of class I DGK in BSC-1 cells results in a >50% reduction in total PA levels, indicating the majority of cellular PA is synthesized by type I DGKs. R59949 is selective for type I DGKs (Jiang *et al.*, 2000), but not other DGK isoforms, suggesting that it is indeed a specific inhibitor of DGK. Under these conditions we detected a reduction in EGFR but not TfR internalization. Using live cell microscopy, we showed that this inhibition in CME correlated with a decrease in CCP initiation and a delayed turnover of productive CCPs. In contrast, inhibition of PLD by either siRNA gene silencing or a chemical inhibitor had the opposite effects. Unexpectedly, PLD inhibition resulted a slight but statistically significant increase in PA levels, an increase in EGFR but not TfR internalization, and a corresponding increase in CCP initiation, and accelerated turnover of both productive and abortive CCPs.

By directly measuring PA, we discovered an unexpected complexity in the relationship between cellular PA levels and the activities of two different classes of enzymes that generate this lipid. Our finding that cellular PA levels *increase* upon inhibition of PLD suggests its participation in a negative-feedback mechanism. In such a scenario, the PA produced by PLD could negatively regulate more efficient, i.e., DGK-dependent, mechanisms of PA production. Interestingly, certain isoforms of DGK are negatively regulated by PA (Suen, 1995; Lung *et al.*, 2009), providing a possible molecular mechanism for this negative feedback. Notably, R59949 only inhibits class I DGKs (Jiang *et al.*, 2000), and a slight increase in PA levels was also detected in cells treated with both FIPI and R59949; thus different classes of DGK (II–V) might be responsible for PLD-regulated PA production. This unexpected complexity reflects the cellular importance for tight regulation of PA biosynthesis and turnover.

The differential effects of DGK and PLD inhibition on EGFR endocytosis correlate with their effects on cellular PA levels. However, we cannot rule out that more subtle biochemical, spatial, or temporal differences in the PA produced by these enzymes also contribute to these differences. For example, each pathway may produce functionally nonequivalent PA based on possible differential acyl chain constituents among substrates for PLD and DGK, which could lead to divergent properties of the PA produced. It is also possible that spatially and/or temporally restricted pools of PA, produced by differentially localized enzymes might contribute to these differential effects. However, there are currently no methods to detect localized PA production at the level of resolution of a CCP. Although our current studies point to a simple and direct correlation between PA levels and EGFR internalization, further studies will be needed to test these possibilities.

Our findings that PLD knockdown accelerates EGFR endocytosis in BSC-1 cells contradict previous studies reporting inhibitory effects of siRNA-mediated gene silencing of PLD on EGFR endocytosis in HEK293 and HeLa cells (Lee *et al.*, 2006; Lee *et al.*, 2009b). Although we cannot explain this discrepancy, our data show that this difference is not a consequence of acute inhibition of PLD, because we obtained similar results either by FIPI treatment or by siRNA gene silencing of PLD. This discrepancy also appears not to be readily attributable to cell type differences, because we were able to observe stimulatory effects of FIPI treatment on EGF uptake in multiple cell lines (data not shown). Thus, although PLD likely has other cellular functions, we conclude that it also serves as a negative regulator of cellular PA levels and of EGFR internalization via CME.

What might be the role of PA in CME? PA, with its small head group, is a cone-shaped lipid that might play a role in curvature generation during initial and/or later stages of CCP assembly and maturation, consistent with the effects we observed on the rates of CCP initiation and turnover of productive CCPs. Alternatively, or in addition, PA, like PIP_2, might play a role in recruiting specific proteins to CCPs. Interestingly, the endocytic scaffolding protein CIN85, which is recruited to ligand-bound EGFR can bind PA (Zhang *et al.*, 2009). Furthermore, Grb2, which is specifically required for EGFR but not TfR internalization (Huang *et al.*, 2004), interacts with the protein mSOS, which is recruited to the plasma membrane after binding to PA (Zhao *et al.*, 2007).

Regardless of the exact function for PA, our results demonstrate that it is not a universally essential component of CME, but is specifically required for internalization of a cargo-selective subset of CCPs. That PLD and DGK have contrasting effects on total cellular PA levels and correspondingly increase or decrease the rate of EGFR uptake suggests that PA levels play a regulatory role for the internalization of a subset of CME-dependent cargo, including ligand-activated signaling receptors such as the EGFR, and potentially also GPCRs (Du *et al.*, 2004; Koch *et al.*, 2004). These findings highlight the importance of lipids in CME and contribute to the understanding of how lipids and lipid dynamics contribute to CCP maturation.

Our findings also add to previous studies that found heterogeneous behavior of and requirements for clathrin-mediated endocytosis governed by the receptors contained therein (Puthenveedu and von Zastrow, 2006; Mettlen *et al.*, 2010). Collectively, they support a model in which diverse receptors differentially utilize subsets of clathrin accessory proteins and/or lipids to create "customized" CCPs and CCVs for transport into the cell.

ACKNOWLEDGMENTS

We thank Dr. Michael Frohman for the kind gift of initial quantities of FIPI. We also thank Allen Liu, Marcel Mettlen, Sylvia Neumann, and Thomas Pucadyil for helpful discussions. This work was supported by National Institutes of Health Grants GM73165 to G.D. and S.L.S. and MH61345 to S.L.S. This is TSRI manuscript no. 20735.

REFERENCES

Bligh, E. G., and Dyer, W. J. (1959). A rapid method of total lipid extraction and purification. Can. J. Biochem. Physiol. *37*, 911–917.

Botelho, R. J., Teruel, M., Dierckman, R., Anderson, R., Wells, A., York, J. D., Meyer, T., and Grinstein, S. (2000). Localized biphasic changes in phosphatidylinositol-4,5-bisphosphate at sites of phagocytosis. J. Cell Biol. *151*, 1353–1368.

Boucrot, E., Saffarian, S., Massol, R., Kirchhausen, T., and Ehrlich, M. (2006). Role of lipids and actin in the formation of clathrin-coated pits. Exp. Cell Res. *312*, 4036–4048.

Cai, J., Abramovici, H., Gee, S. H., and Topham, M. K. (2009). Diacylglycerol kinases as sources of phosphatidic acid. Biochim. Biophys. Acta *1791*, 942–948.

Chomczynski, P., and Mackey, K. (1995). Short technical reports. Modification of the TRI reagent procedure for isolation of RNA from polysaccharide- and proteoglycan-rich sources. Biotechiques *19*, 942–945.

Collinet, C., *et al.* (2010). Systems survey of endocytosis by multiparametric image analysis. Nature *464*, 243–249.

Conner, S. D., and Schmid, S. L. (2003a). Differential requirements for AP-2 in clathrin-mediated endocytosis. J. Cell Biol. *162*, 773–779.

Conner, S. D., and Schmid, S. L. (2003b). Regulated portals of entry into the cell. Nature *422*, 37–44.

Du, G., Huang, P., Liang, B. T., and Frohman, M. A. (2004). Phospholipase D2 localizes to the plasma membrane and regulates angiotensin II receptor endocytosis. Mol. Biol. Cell *15*, 1024–1030.

Exton, J. H. (1997). Phospholipase D: enzymology, mechanisms of regulation, and function. Physiol. Rev. *77*, 303–320.

Haucke, V. (2005). Phosphoinositide regulation of clathrin-mediated endocytosis. Biochem. Soc. Trans. *33*, 1285–1289.

Huang, F., Khvorova, A., Marshall, W., and Sorkin, A. (2004). Analysis of clathrin-mediated endocytosis of epidermal growth factor receptor by RNA interference. J. Biol. Chem. *279*, 16657–16661.

Jiang, X., Huang, F., Marusyk, A., and Sorkin, A. (2003). Grb2 regulates internalization of EGF receptors through clathrin-coated pits. Mol. Biol. Cell *14*, 858–870.

Jiang, Y., Sakane, F., Kanoh, H., and Walsh, J. P. (2000). Selectivity of the diacylglycerol kinase inhibitor 3-[2-(4-[bis-(4-fluorophenyl)methylene]-1-piperidinyl)ethyl]-2, 3-dihydro-2-thioxo-4(1H)quinazolinone (R59949) among diacylglycerol kinase subtypes. Biochem. Pharmacol. *59*, 763–772.

Jost, M., Simpson, F., Kavran, J. M., Lemmon, M. A., and Schmid, S. L. (1998). Phosphatidylinositol-4,5-bisphosphate is required for endocytic coated vesicle formation. Curr. Biol. *8*, 1399–1402.

Kawasaki, T., Kobayashi, T., Ueyama, T., Shirai, Y., and Saito, N. (2008). Regulation of clathrin-dependent endocytosis by diacylglycerol kinase delta: importance of kinase activity and binding to AP2alpha. Biochem. J. *409*, 471–479.

Koch, T., Brandenburg, L., Liang, Y., Schulz, S., Beyer, A., Schröder, H., and Höllt, V. (2004). Phospholipase D2 modulates agonist-induced mu-opioid receptor desensitization and resensitization. J. Neurochem. *88*, 680–688.

Lamaze, C., and Schmid, S. L. (1995). Recruitment of epidermal growth factor receptors into coated pits requires their activated tyrosine kinase. J. Cell Biol. *129*, 47–54.

Lee, C. S., Kim, I. S., Park, J. B., Lee, M. N., Lee, H. Y., Suh, P. G., and Ryu, S. H. (2006). The phox homology domain of phospholipase D activates dynamin GTPase activity and accelerates EGFR endocytosis. Nat. Cell Biol. *8*, 477–484.

Lee, C. S., Kim, K. L., Jang, J. H., Choi, Y. S., Suh, P., and Ryu, S. H. (2009a). The roles of phospholipase D in EGFR signaling. Biochim. Biophys. Acta *1791*, 862–868.

Lee, J. S., Kim, I. S., Kim, J. H., Cho, W., Suh, P. G., and Ryu, S. H. (2009b). Determination of EGFR endocytosis kinetic by auto-regulatory association of PLD1 with mu2. PLoS ONE *4*, e7090.

Liu, Y., Surka, M. C., Schroeter, T., Lukiyanchuk, V., and Schmid, S. L. (2008). Isoform and splice-variant specific functions of dynamin-2 revealed by analysis of conditional knock-out cells. Mol. Biol. Cell *19*, 5347–5359.

Loerke, D., Mettlen, M., Yarar, D., Jaqaman, K., Jaqaman, H., Danuser, G., and Schmid, S. L. (2009). Cargo and dynamin regulate clathrin-coated pit maturation. PLoS Biol. *7*, e57.

Lung, M., Shulga, Y. V., Ivanova, P. T., Myers, D. S., Milne, S. B., Brown, H. A., Topham, M. K., and Epand, R. M. (2009). Diacylglycerol kinase epsilon is selective for both acyl chains of phosphatidic acid or diacylglycerol. J. Biol. Chem. *284*, 31062–31073.

Mettlen, M., Loerke, D., Yarar, D., Danuser, G., and Schmid, S. L. (2010). Cargo- and adaptor-specific mechanisms regulate clathrin-mediated endocytosis. J. Cell Biol. *188*, 919–933.

Mettlen, M., Stoeber, M., Loerke, D., Antonescu, C. N., Danuser, G., and Schmid, S. L. (2009). Endocytic accessory proteins are functionally distinguished by their differential effects on the maturation of clathrin-coated pits. Mol. Biol. Cell *20*, 3251–3260.

Morita, S., Ueda, K., and Kitagawa, S. (2009). Enzymatic measurement of phosphatidic acid in cultured cells. J Lipid Res. *50*, 1945–1952.

Motley, A., Bright, N. A., Seaman, M. N., and Robinson, M. S. (2003). Clathrin-mediated endocytosis in AP-2-depleted cells. J. Cell Biol. *162*, 909–918.

Padrón, D., Tall, R. D., and Roth, M. G. (2006). Phospholipase D2 is required for efficient endocytic recycling of transferrin receptors. Mol. Biol. Cell *17*, 598–606.

Puthenveedu, M. A., and von Zastrow, M. (2006). Cargo regulates clathrin-coated pit dynamics. Cell *127*, 113–124.

Rozen, S., and Skaletsky, H. (2000). Primer3 on the WWW for general users and for biologist programmers. Methods Mol Biol. *132*, 365–386.

Schmid, E. M., and McMahon, H. T. (2007). Integrating molecular and network biology to decode endocytosis. Nature *448*, 883–888.

Scott, S. A., Selvy, P. E., Buck, J. R., Cho, H. P., Criswell, T. L., Thomas, A. L., Armstrong, M. D., Arteaga, C. L., Lindsley, C. W., and Brown, H. A. (2009). Design of isoform-selective phospholipase D inhibitors that modulate cancer cell invasiveness. Nat. Chem. Biol. *5*, 108–117.

Shen, Y., Xu, L., and Foster, D. A. (2001). Role for phospholipase D in receptor-mediated endocytosis. Mol. Cell. Biol. *21*, 595–602.

Sigismund, S., Argenzio, E., Tosoni, D., Cavallaro, E., Polo, S., and Di Fiore, P. P. (2008). Clathrin-mediated internalization is essential for sustained EGFR signaling but dispensable for degradation. Dev. Cell *15*, 209–219.

Sorkin, A., and Goh, L. K. (2009). Endocytosis and intracellular trafficking of ErbBs. Exp. Cell Res. *315*, 683–696.

Stauffer, T. P., Ahn, S., and Meyer, T. (1998). Receptor-induced transient reduction in plasma membrane PtdIns(4,5)P2 concentration monitored in living cells. Curr. Biol. *8*, 343–346.

Su, W., Yeku, O., Olepu, S., Genna, A., Park, J. S., Ren, H., Du, G., Gelb, M. H., Morris, A. J., and Frohman, M. A. (2009). 5-Fluoro-2-indolyl des-chlorohalopemide (FIPI), a phospholipase D pharmacological inhibitor that alters cell spreading and inhibits chemotaxis. Mol. Pharmacol. *3*, 437–446.

Suen, R. (1995). Arachidonoyl-diacylglycerol kinase. J. Biol. Chem. *270*, 28647–28653.

Tosoni, D., Puri, C., Confalonieri, S., Salcini, A. E., De Camilli, P., Tacchetti, C., and Di Fiore, P. P. (2005). TTP specifically regulates the internalization of the transferrin receptor. Cell *123*, 875–888.

Yanase, Y., Carvou, N., Frohman, M. A., and Cockcroft, S. (2010). Reversible bleb formation in mast cells stimulated with antigen is Ca^{2+}/calmodulin-dependent and bleb size is regulated by ARF6. Biochem. J. *425*, 179–193.

Yarar, D., Waterman-Storer, C. M., and Schmid, S. L. (2005). A dynamic actin cytoskeleton functions at multiple stages of clathrin-mediated endocytosis. Mol. Biol. Cell *16*, 964–975.

Zhang, J., Zheng, X., Yang, X., and Liao, K. (2009). CIN85 associates with endosomal membrane and binds phosphatidic acid. Cell Res. *19*, 733–746.

Zhao, C., Du, G., Skowronek, K., Frohman, M. A., and Bar-Sagi, D. (2007). Phospholipase D2-generated phosphatidic acid couples EGFR stimulation to Ras activation by Sos. Nat. Cell Biol. *9*, 706–712.

Zoncu, R., Perera, R. M., Sebastian, R., Nakatsu, F., Chen, H., Balla, T., Ayala, G., Toomre, D., and De Camilli, P. V. (2007). Loss of endocytic clathrin-coated pits upon acute depletion of phosphatidylinositol 4,5-bisphosphate. Proc. Natl. Acad. Sci. USA *104*, 3793–3798.

van Rheenen, J., Song, van Roosmalen, X., W., Cammer, M., Chen, X., Desmarais, V., Backer, J. M., Eddy, R. J., and Condeelis, J. S. (2007). EGF-induced PIP2 hydrolysis releases and activates cofilin locally in carcinoma cells. J. Cell Biol. *179*, 1247–1259.

van den Bout, I., and Divecha, N. (2009). PIP5K-driven PtdIns(4,5)P2 synthesis: regulation and cellular functions. J. Cell Sci. *122*, 3837–3850.